JOURNAL OF GEOPHYSICAL RESEARCH, VOL. 105, NO. D16, PAGES 20,707–20,724, AUGUST 27, 2000

# Effect of meteorology and air pollutant transport on ozone episodes at a subtropical coastal Asian city, Hong Kong

C. Y. Chan and L. Y. Chan

Environmental Engineering Unit, Department of Civil and Structural Engineering, Hong Kong Polytechnic University, Hung Hom, Hong Kong

**Abstract.** Hong Kong is a subtropical coastal city situated at the rapid urbanizing and industrializing region of South China. High frequencies of elevated ozone are found in various remote, rural, and metropolitan districts of Hong Kong. Meteorological conditions related to synoptic-scale flow pattern, mesoscale weather phenomenon, and local micrometeorology have strong effects on the pollutant transport to South China and the occurrence of ozone episodes in Hong Kong. The transport processes and the source regions of ozone are analyzed with the combined use of surface pressure patterns, streamline charts and prevalent winds, and with representative episodes. The synoptic meteorological conditions can be classified into nine patterns. The patterns associated with winter monsoon and traveling cyclones are found to be most conducive to the occurrence of ozone episodes. Long-range transport of ozone with enhanced CO level from the aged continental air accompanying northeast monsoon contributes to substantial cases of episodes, which are especially noticeable in the upwind remote areas. These episodes feature consistently high ozone at night in the remote station and early morning peaks in the metropolitan stations. The possible source regions of this ozone may include Asian continent, the coastal areas of Mainland China, southern Japan, and Taiwan. This high inflow of background ozone together with elevated ozone enhanced by the channeling effect, and local transport causes the highest frequencies of ozone episodes in the downwind western side of the territory. The short-range transport of ozone and pollutants from the industrial and urban centers in the Pearl River Delta region and Guangdong Province in southern China is another source of ozone. When transported ozone is being superimposed on ozone formed from local sources, territory-wide and extremely high concentration episodes are found. Our meteorological and ozone episode diagnosis have also demonstrated that the 'background' outflow of Asian pollutants can be significantly modified on its way to the Pacific Ocean when passing through the fast growing Pearl River Delta cities such as Hong Kong.

## 1. Introduction

Elevated ozone is a cause of citizen's concern. Photochemical ozone formation involving its chemical precursors (mainly VOC and $NO_x$) and ozone transport from upwind aged air are the two major anthropogenic sources of ozone in urban and rural areas [*Colbeck and Harrision*, 1985; *Logan*, 1989; *Akimoto et al.*, 1996]. In the abundance of precursors, elevated photochemical formation and accumulation of ozone are common phenomena, and ozone may reach an episodic concentration level. Ozone pollution may not simply confined to the anthropogenic source region but can spread to large geographical extent due to different scales of transportation of pollution plumes from the source region. Its impact had been reported to reach a regional and even continental scale in Asia, Europe, and North America [*Liu et al.*, 1999; *Colbeck and Harrision*, 1985; *Parrish et al.*, 1993; *Jacob et al.*, 1999]. Ozone in high concentration level can impose direct adverse effects on human health and the ecosystem [*Lippmann*, 1991; *National Research Council*, 1991].



Paper number 2000JD900140
0148-0227/00/2000JD900140$09.00

In the rapid industrializing and urbanizing eastern Asian region and especially in South China, unfortunately, measurement of ozone is comparatively limited. Hence it is more difficult to evaluate the extent of ozone pollution in this region. Hong Kong (22°N, 114°E) is a subtropical and coastal city in South China located on the eastern Asian edge between the Asian continent, the North Pacific Ocean, and the South China Sea. South China including the Pearl River Delta (PRD) region of Guangdong Province (Figure 1) and the territory of Hong Kong is one of the fastest growing regions in the world with rapid industrial and urban development. The huge amount of pollutant emissions from various anthropogenic sources are a potential health risk to the respective 6.8 million people living in Hong Kong and 70 million people living in its neighboring cities in Guangdong Province. The coastal region of southeast China and Hong Kong is a transition zone of East Asian monsoon system, where different air masses meet under the control of large-scale monsoon winds. Such monsoon flows put South China and Hong Kong as a receptor of the large amounts of pollutant emissions in the East Asian Pacific Rim (EAPR). On the contrary, the pollutant outflows from the PRD cities and Hong Kong are also expected to affect the atmospheric environment in EAPR as well as the West Asian Pacific Rim (WAPR).

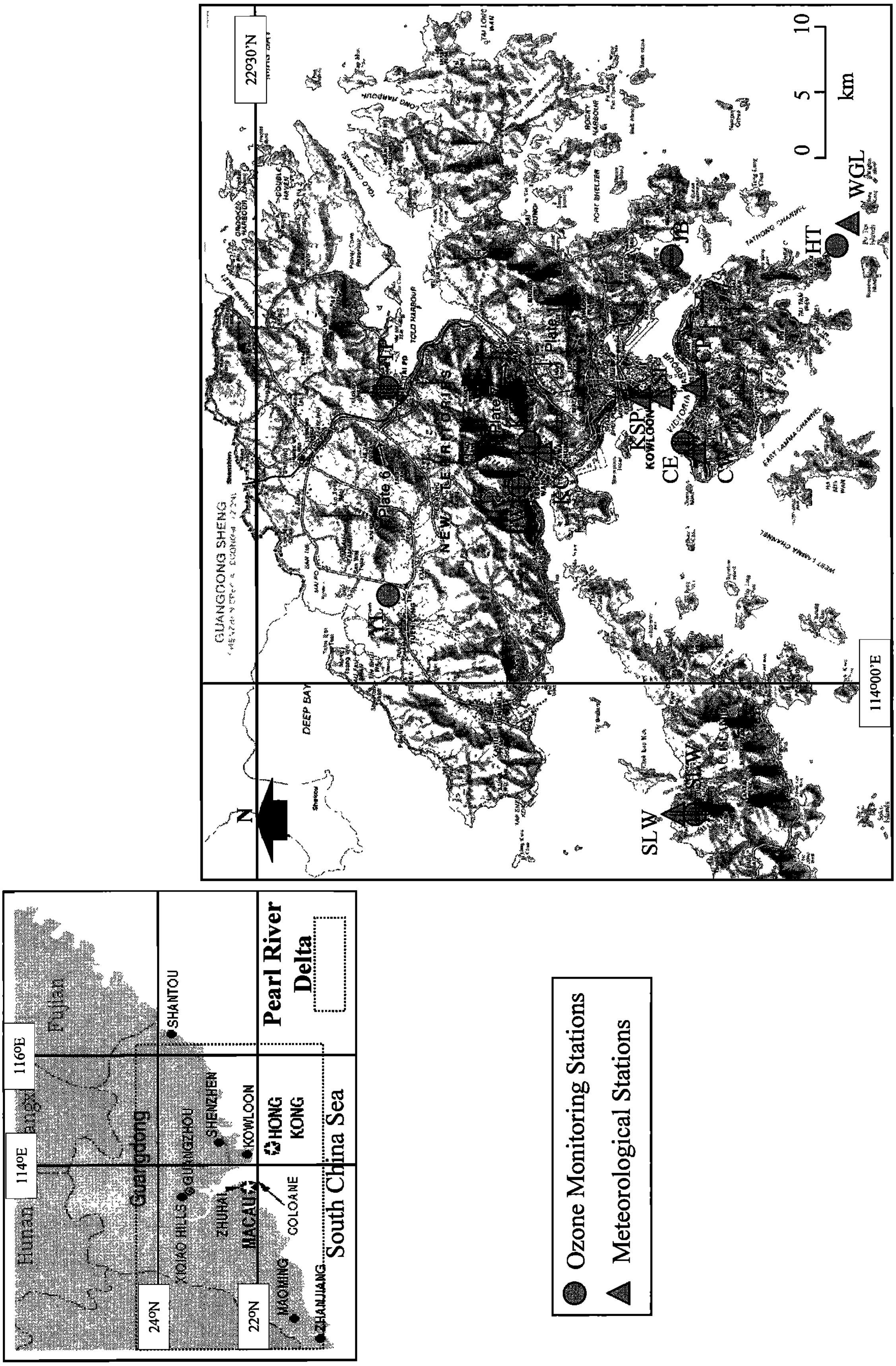


**Figure 1.** Geographical locations of Hong Kong and the neighboring cities, and the ozone and meteorological monitoring stations in Hong Kong.

The air transport to South China and Hong Kong is complicated by the complex local meteorology induced by topography and land-sea interaction in the coast of South China and within the territory of Hong Kong. *Jaffe et al.* [1999] had shown that there were cases of transport of Asian air pollution to North America in approximately 6 days. These Asian anthropogenic emissions significantly impact the concentrations of a large number of atmospheric species in the air arriving to North America. *Jacob et al.* [1999] had also discussed the effect of rising Asian emissions on surface ozone to the United States. Trace gas measurements from the background air quality monitoring station of the Hong Kong Polytechnic University (HKPolyU) revealed that high and variable levels of trace gases (ozone, CO, $NO_y$ and $SO_2$) were associated with continental outflow reaching Hong Kong. The indication is that the air masses were inhomogeneous in nature with contributions of pollutants from different source regions [*Wang et al.*, 1997]. In earlier papers we reported that lower tropospheric and surface ozone in Hong Kong had a unique bimodal seasonal variation pattern [*Chan et al.*, 1998a, b]. The monthly average ozone concentrations showed a major peak in autumn and a trough in summer. Utilizing information on ozone precursor levels, production, and transport of ozone, we proposed that the alternation of prevalent oceanic and continental air masses plus the climatic system associated with the Asian monsoon system were the governing factors for the observed surface ozone variations [*Chan et al.*, 1998a]. In particular, the continental outflow of aged air masses to the South China Sea in the Pacific associated with the winter monsoon was responsible for the transport of anthropogenic air pollutants from the industrial and urban centers of Guangdong Province to Hong Kong. We also pointed out that favorable weather and meteorological conditions in southeast China in autumn were crucial factors for the elevated ozone formation and observed ozone peaks in that season. In this study, we have analyzed the photochemical ozone episodes at various urban, rural, and background environments of Hong Kong with emphasis on assessing the effects of meteorology and air pollutant transport on the occurrence of ozone episodes.

## 2. Data Sources

Surface ozone and precursors ($NO_x$ and CO) data from air quality monitoring stations of the Environmental Protection Department (EPD) of Hong Kong and the HKPolyU background air quality station were used in our analysis. They represent a comprehensive and valuable database in South China. We focused on data from eight monitoring stations: remote area (Hok Tsui, HT), rural area (Sha Lo Wan, SLW), subrural area (Junk Bay, JB), urban area (Centralwest, CW), industrial areas (Kwai Chung, KC and Tsuen Wan, TW), and new towns (Yuen Long, YL and Tai Po, TP). The monitoring locations are shown in Figure 1. Table 1 summarizes the characteristics of the monitoring stations and the periods of ozone measurements used for analysis in this study. The data from HT were such that they represented measurement in 1994, while those from SLW and YL were in 1996. There is a short break from late July to late August 1994 in HT. For the other stations the data represented periodic measurements from 1990 to 1996. We had tried to fully utilize the available data for analysis, but the reader needs to note the discrepancies in the available data set.

For all EPD stations, the gaseous pollutants were measured by either the U.S. Environmental Protection Agency (EPA) standard or reference methods. Ozone was measured based on UV light absorption principle (Dasibi 1003-RS and TECO 49), and CO was measured by nondispersive infrared analyzer (TECO 48). $NO_x$ was measured by duel-channel chemiluminescent analyzer for the continuous detection of NO and $NO_2$ (TECO 42). The readers are reminded that the $NO_2$ measurement by chemiluminescent method has potential interference from nitric acid, peroxyacetyl nitrate (PAN) and other atmospheric nitrates. Quality assurance and quality control programs similar to those required by the U.S. EPA were adopted by EPD [*EPD*, 1994]. In the HKPolyU background station a stricter quality assurance and control requirement was implemented, and a detailed description is available in literature [*Wang et al.*, 1997; *Chan et al.*, 1998a].

Meteorological data extracted from the daily weather maps and automatic meteorological stations of the Hong Kong Observatory were used for analysis. The locations of these stations are shown in Figure 1. Table 1a summarizes the characteristics of the monitoring stations and the parameters used, while Table 1b gives the characteristics of the meteorological stations. In particular, the wind speed and direction measured in Waglan Island next to HT station are adopted (Figure 1). The data recorded in this station are more representative of the prevailing winds of Hong Kong since the station is far away from any geographical barrier. In addition, daily surface streamline charts (1000 hPa) supplied by the NASA Global Tropospheric Experiment Project Office were used in the analysis (available at http://www-gte.larc.nasa.gov). Two streamline charts per days at 0000 and 1200 UTC were generated and plotted upon the regions in the periods of interest. These charts or plots were derived from the National Center for Environmental Prediction global data sets at 2.5° resolution. In this study, we are interested in the region with latitude from 0° to 45°N and longitude from 95° to 145°E.

## 3. Methodology

Synoptic meteorological patterns as well as local micrometeorology are used to link together ozone transport and photochemical ozone production for the understanding of

**Table 1a.** Ozone Monitoring Stations in Hong Kong

| Stations | Abbreviation | Aboveground, m | Characteristics of the Stations | Pollutants | Data Available |
|---|---|---|---|---|---|
| Hok Tsui | HT | 6 | rural: remote | $O_3$, CO | Jan.-Dec. 1994 |
| Sha Lo Wan | SLW | 12 | rural: with new development | $O_3$, $NO_x$ | Jan.-Dec. 1996 |
| Junk Bay | JB | 13 | subrural: with some industries | $O_3$, $NO_x$ | Jan. 1990 to Dec. 1992 |
| Centralwest | CW | 18 | urban: commercial/ residential | $O_3$, $NO_x$ | Jan. 1990 to Dec. 1996 |
| Kwai Chung | KC | 25 | urban: industrial/residential | $O_3$, $NO_x$, CO | Jan. 1990 to Dec. 1996 |
| Tsuen Wan | TW | 17 | urban: industrial/residential | $O_3$, $NO_x$ | Aug. 1990 to Jul. 1994 |
| Tai Po | TP | 25 | new town: industrial/residential | $O_3$, $NO_x$ | Feb. 1990 to Jan. 1993 |
| Yuen Long | YL | 25 | new town: industrial/residential | $O_3$, $NO_x$ | Jan. 1996 to Dec. 1996 |

**Table 1b.** Meteorological Stations in Hong Kong

| Stations | Abbreviation | Aboveground, m | Characteristics of the Stations | Parameters | Data Available |
|---|---|---|---|---|---|
| Waglan Island | WGL | 55 | rural: remote | wind | Jan. 1990 to Dec. 1996 |
| Sha Lo Wan | SLW | 71 | rural: with new development | wind | Jan. 1990 to Dec. 1996 |
| Star Ferry | SF | 18 | urban: commercial | wind | Jan. 1990 to Dec. 1996 |
| Central | CE | 17 | urban: commercial/ residential | wind | Jan. 1990 to Dec. 1996 |
| Kwai Chung | KC | 63 | urban: industrial/residential | wind | Jan. 1990 to Dec. 1996 |
| Central Plaza | CP | 378 | urban: commercial | wind | Jan. 1990 to Dec. 1996 |
| King's Park | KSP | 65 | urban: commercial/residential | wind, temperature, solar radiation | Jan. 1990 to Dec. 1996 |

the occurrence of ozone episodes. We first identify the meteorological events, that is those repeating themselves during episodes, and then explain the relative photochemical formation processes leading to the ozone episodes. With such information, we would further identify the major pollutant source regions and the corresponding transport patterns.

Studies had shown that average ozone levels in urban areas are usually lower than their counterparts in the rural and subrural areas [*Angle and Sandhu*, 1986; *Bower et al.*, 1989] due to the titration effect of nitric oxide, especially those emitted from automobiles, on ozone. Therefore it is important for us to select appropriate episodic concentration levels that can apply to both rural and urban areas. We use the exceedence level in daily maximum hourly ozone concentration as the selection criteria. Ozone episode days are defined as the ones with at least one hourly average ozone concentration exceeding 60 ppb. These days are further grouped according to whether the hourly concentration exceeded 60, 80, 100, and 122 ppb. These thresholds are selected with reference to the relevant standards and guidelines required or recommended by the World Health Organization, the United Kingdom Photochemical Oxidant Review Group [*PORG*, 1990], and the Air Quality Objectives of Hong Kong (AQOHK).

Synoptic patterns classified according to pressure patterns and air trajectories with respect to air mass flows were commonly used in ozone study [*Hanna and Chang*, 1995; *Moody et al.*, 1995; *Fast and Berkowitz*, 1997]. However, the rough nature of the pressure pattern denoted by daily weather map and the inherited uncertainty of air trajectory have hampered the effectiveness of these approaches for the study of ozone in regions with complex emission settings and transport patterns. In our study, we use surface pressure patterns denoted by daily weather maps, streamline charts, and surface prevalent winds. This approach not only provides a closer look at the synoptic-scale airflow patterns and mesoscale weather phenomena but also utilizes the associated local micrometeorological conditions. The major pressure patterns and their transient features are determined from the daily weather maps. These include centers of anticyclone, cyclone, and tropical storm, the location of the ridge, axis of trough, and front. The surface pressure patterns have shown to be useful in determining the general movements of air masses in the east Asian region [*Heywood*, 1953; *Chin*, 1986; *Chan et al.*, 1998a] and elsewhere [*PORG*, 1990; *NRC*, 1991, and references therein]. Chin had illustrated that it is possible to determine the major surface air flow into the territory in different seasons according to the surface pressure pattern as Hong Kong is far enough from the equator. We have also demonstrated that the seasonal variation of ozone concentration is highly related to the seasonal changes of the surface pressure patterns [*Chan et al.*, 1998a]. However, the synoptic air mass flows are subject to modifications by smaller-scale processes that are likely to occur in coastal areas of South China and Hong Kong, where the airflow patterns are complicated by the existence of land and sea interaction, and complex terrain [*Yeung et al.*, 1990].

Our experiences show that when we solely rely on the surface pressure pattern, we over simplify the synoptic flow patterns due to the ignoring of the smaller-scale processes. This situation is frequent in winter when the transport of continental air masses and pollutants are important. The coexistence of several well-defined surface pressure patterns has shown to be problematic for classification based on daily weather maps alone. This is because it is difficult to determine which pattern has a dominant influence. Similar confusion may also occur in summer when the surface pressure patterns are less intensive and show less persistence due to the weaker strength of the summer monsoon. The addition of the better time resolution streamline charts and prevailing winds helps us to determine more clearly the dominant paths of the air mass flows and the recent history of air reaching Hong Kong. Subsequently, it allows us to better pinpoints the source regions and characterizes the transport of ozone and precursors. The major inflow regions are classified according to the directions as determined by the eight point compass settings centered at Hong Kong.

## 4. Result

### 4.1. General and Spatial Characteristics of Ozone Episodes

Table 2 summarizes the total number of days with maximum hourly ozone concentration exceeding 60, 80, 100, and 122 ppb levels together with the maximum hourly and daily ozone concentrations recorded by the monitoring stations. A total of 373 station days covering the period from 1990 to 1996 were identified with at least an hourly ozone concentration greater than 60 ppb. The period covered was different for different stations due to the availability of data (Table 1). The number of station days with hourly ozone concentration greater than the hourly ozone AQOHK (122 ppb) and 100 ppb level were 11 and 43, respectively. There were 107 station days exceeding the 80 ppb level.

To facilitate our comparison on the spatial occurrence of episodes, we also summarize the number of episodes per year recorded in each station in Table 2. Higher frequencies of ozone episodes were found in the upwind remote districts on the eastern side, and especially in the downwind rural districts on the western and northwestern sides of the territory. This is reflected by the high numbers of episodes in the HT, SLW, and YL stations, which occurred in a single year. In SLW there were 5, 21, and 51 episodes with ozone concentration

**Table 2.** Total and Number of Occurrence of Ozone Episodes per Year in Different Exceeding Levels and the Maximum Daily and Hourly Ozone Concentrations in Each Station

| | Total Number. of Episodes Exceedance Levels, ppb | | | | Number of Episodes per Year Exceedance Levels, ppb | | | | Maximum concentration, ppb | | |
|---|---|---|---|---|---|---|---|---|---|---|---|
| | 60 | 80 | 100 | 122 | 60 | 80 | 100 | 122 | Daily | Hourly | Data Available |
| Hok Tsui | 72 | 9 | 5 | 1 | 72.0 | 9.0 | 5.0 | 1.0 | 73.2 | 162.0 | Jan.-Dec. 1994 |
| Sha Lo Wan | 111 | 51 | 21 | 5 | 111.0 | 51.0 | 21.0 | 5.0 | 51.8 | 156.8 | Jan.-Dec. 1996 |
| Junk Bay | 22 | 8 | 1 | 0 | 11.0 | 4.0 | 0.5 | 0.0 | 58.5 | 114.9 | Jan. 1990 to Dec. 1992 |
| Centralwest | 64 | 16 | 8 | 1 | 10.1 | 2.7 | 1.3 | 0.2 | 61.5 | 159.6 | Jan. 1990 to Dec. 1996 |
| Kwai Chung | 50 | 10 | 5 | 3 | 8.3 | 1.7 | 0.8 | 0.5 | 70.7 | 152.3 | Jan. 1990 to Dec. 1996 |
| Tsuen Wan | 15 | 3 | 0 | 0 | 3.8 | 0.8 | 0.0 | 0.0 | 33.5 | 98.1 | Aug. 1990 to Jul. 1994 |
| Tai Po | 2 | 0 | 0 | 0 | 0.7 | 0.0 | 0.0 | 0.0 | 10.2 | 78.3 | Feb. 1990 to Jan. 1993 |
| Yuen Long | 37 | 10 | 3 | 1 | 37.0 | 10.0 | 3.0 | 1.0 | 43.2 | 136.2 | Jan. 1996 to Dec. 1996 |
| Total | 373 | 107 | 43 | 11 | ----- | ----- | ----- | ----- | 73.2 | 162.0 | ------ |

greater than 122, 100, and 80 ppb, respectively in 1996. In YL there were 1, 3, and 10 days with ozone concentration greater than 122, 100, and 80 ppb, respectively in 1996. The respective values for HT in 1994 were 1, 5, and 9. In other stations, especially those in urban and industrial areas and early years of the study period from 1990 to 1993, the occurrence of episode per year was much lower. The apparent low frequency of episode over the 7-year study period is due to the low occurrence of ozone episodes in the urban and industrial stations especially from 1990 to 1993 and the relatively limited available data from the remote, rural and new town stations. However, based on more recent data covering 1994 to 1996 from the remote, rural, and new town stations, we see that elevated ozone pollution is quite serious. In fact, the 6 days with ozone concentration greater 122 ppb occurred in these periods.

High concentration with maximum hourly ozone concentration exceeding 100 ppb was found in most areas. The maximum hourly concentration recorded in remote (HT), rural (SLW), subrural (JB), urban commercial (CW), industrial (KC and TW) stations, and new towns (TP and YL) were 162, 156.8, 114.9, 159.6, 152.3, and 136.2 ppb, respectively. The respective maximum daily average concentrations of these stations were 73.2, 51.8, 58.3, 61.5, 70.7, and 43.2 ppb. These findings suggest that ozone pollution is widespread in the whole territories of Hong Kong, and is especially serious in the rural and remote districts.

### 4.2. Relations Between Synoptic Meteorology and Ozone Episodes

There were 186, 58, 33, and 6 individual days with at least one station experiencing daily maximum ozone

**Table 3.** Synoptic Meteorology and Weather Conditions of Ozone Episodes

| Types | Dominant Surface Pressure Patterns | Major Flow Patterns and Surface Winds in Hong Kong | Weather and Atmospheric Conditions | Period of Frequent Occurrence |
|---|---|---|---|---|
| Northerly (N) | continental anticyclone over northwestern China | straight northerly anticyclonic flow from Mainland China as north or northeast winds | dry, clear sky and occasionally cold and strong wind | Dec. to March |
| Weak northerly (wN) | moderate or weak continental anticyclone over northwestern China | weak and straight northerly anticyclonic flow from Mainland China as weak north or northwest wind | dry and clear sky | Oct. to early Dec. |
| North-easterly (NE) | continental anticyclone over northeastern China, East China Sea, and southern Japan | northeasterly anticyclonic flow from East China Sea and Taiwan Straits as northeast and east winds | dry, clear sky and long sunshine hours | late Sept. to mid. Mar. |
| Easterly or southeasterly (E) | anticyclone centered east of 130° E and north of 20° N | easterly or northeasterly anticyclonic flow as east or southeast winds | fairly long sunshine hours | mid. Apr. to mid May |
| Trough (T) | low-pressure trough with axis extending approximately east-west over south China | northerly anticyclonic flow to the north of trough and easterly cyclonic flow to the south; wind is variable | low wind and stagnant atmosphere | late May to early Jun.; mid. Aug. to mid. Sept. |
| Southerly or southwesterly (S) | Quasi-stationary low-pressure area over Asian continent | cyclonic flow from the South China Sea as south or southwest wind | high temperature and strong solar radiation | June. to Aug. |
| Pacific ridge (P) | ridge of Pacific high-pressure extending to Taiwan and southeastern China | straight flow from the Pacific Ocean as east or southeast winds | high temperature and strong solar radiation | June. to Aug. |
| High-pressure cell (H) | weak high pressure cell over south China | weak anticyclonic flow with weak surface winds | clear sky, long sunshine hours and low wind | early Sept.; late April to late May |
| Cyclone (C) | Hong Kong within circulation of a traveling cyclone | cyclonic flow as north or northwest winds | low-level inversion, hot, clear sky, and long sunshine hour | May to early Dec. |

**Table 4.** Number of Ozone Episodes in Different Exceeding Levels and the Maximum Daily and Hourly Ozone Concentrations in Each Synoptic Type

| | Exceedance Levels, ppb | | | | Maximum Concentration, ppb | |
|---|---|---|---|---|---|---|
| | 60 | 80 | 100 | 122 | Daily | Hourly |
| NE | 67 | 18 | 7 | 1 | 43.4 | 124.7 |
| C | 43 | 21 | 13 | 4 | 73.2 | 162.0 |
| E | 23 | 3 | 1 | 1 | 53.3 | 141.5 |
| N | 21 | 7 | 5 | 0 | 47.8 | 114.4 |
| wN | 18 | 5 | 5 | 0 | 48.6 | 119.7 |
| T | 7 | 1 | 1 | 0 | NV* | 104.7 |
| H | 4 | 2 | 1 | 0 | 60.0 | 105.7 |
| P | 3 | 1 | 0 | 0 | 58.0 | 77.8 |
| S | 1 | 0 | 0 | 0 | 12.7 | 63.5 |
| Total | 187 | 58 | 33 | 6 | 73.2 | 162.0 |

*NV stands for not valid data.

concentrations greater than 60, 80, 100, and 122 ppb level, respectively. We classified the meteorology of ozone episodes into nine main types using information provided by flow patterns deduced from the surface pressure patterns, streamline charts, and prevalent winds. They are northerly (N), weak northerly (wN), northeasterly (NE), easterly (E), Pacific ridge (P), cyclone (C), high pressure cell (H), trough (T), and southerly (S). A summary describing these synoptic patterns in terms of the mesoscale and local-scale flow patterns as demonstrated by the streamlines and surface wind in South China and Hong Kong is given in Table 3. Also included are the periods of dominance of these patterns and the special features of the weather and atmospheric conditions, which lead to the occurrence of the ozone episode days.

Synoptic patterns N, wN, NE, and E are the major features of the winter monsoon of the East Asian monsoon system which occurs dominantly from early autumn to late spring (September to May). These patterns are associated with the buildup of a high-pressure system over the central Asian region, which brings in continental or modified continental air masses from northwestern China through central and mainland China to the coastal areas of southeast China and Hong Kong. Synoptic patterns P, T, and S are the major features of the summer monsoon occurring in summer from early May to late August. The patterns, which are formed from the development of quasi-stationary low pressure over the central Asian region cause inflow of maritime air masses from the tropical and equatorial regions through western Pacific Ocean and South China Sea to southeast China and Hong Kong. The incursion of tropical cyclones (type C) may occur in any month from May to December. Type H can be regarded as an exceptional pattern, which is associated with the southward movement of a weak continental pressure cell that covers the vicinity of Hong Kong. It may also be formed as a result of the rapid change of the major surface circulation. It seldom lasts for a long period of time. The last two synoptic patterns cause a temporal cutting off of the prevalent wind from reaching the region.

Table 4 summarizes the frequency distribution of ozone episodes according to the synoptic types and exceedence

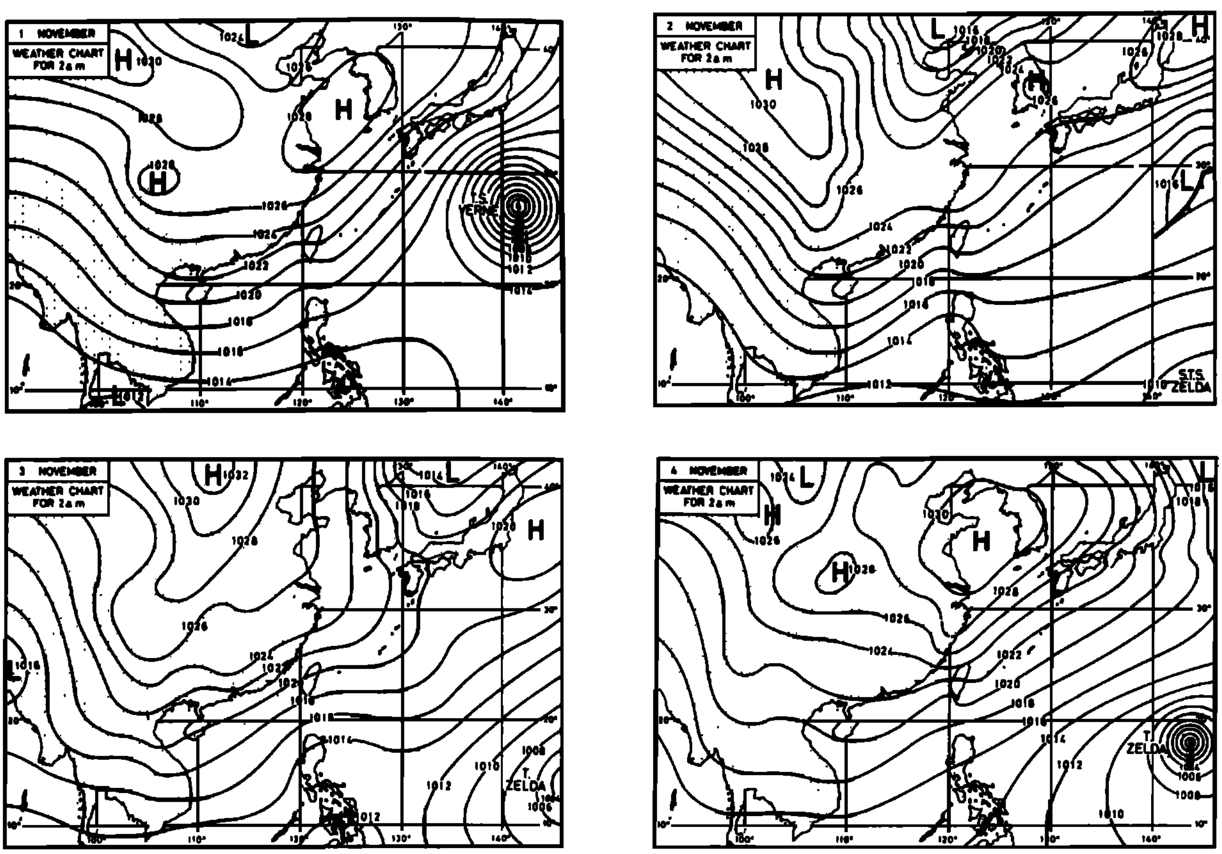


**Figure 2a.** The daily weather maps from November 1 to 4, 1994.

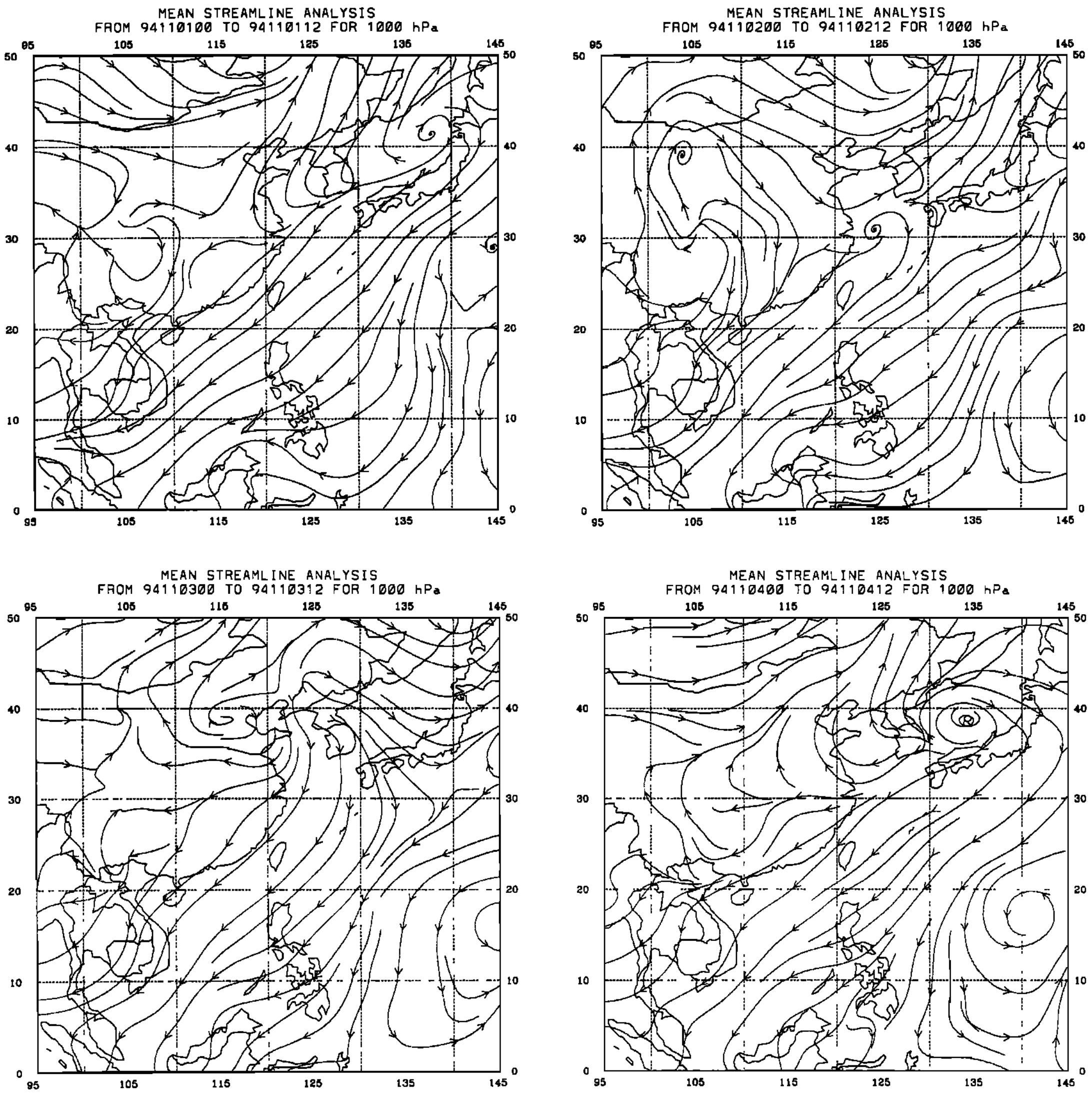


**Figure 2b.** Same as Figure 2a, but for the streamline charts.

levels. The relevant maximum hourly and daily ozone concentration in each synoptic type are also included. The synoptic types associated with the winter monsoon contribute to a higher number and percentage of ozone episode. It is followed by synoptic type C. Relatively few cases of episodes are with the summer monsoon types. Scarcely few episodes are with synoptic type H. It is found that high concentration episodes (>80 ppb) occurred in most synoptic types. In terms of frequency and maximum hourly concentration, noticeably higher numbers of elevated concentration level of episodes are associated with type C and the winter monsoon types. Most episodes of the summer monsoon types and H are of lower concentration level. There were a total of 129, 33, 18, and 2 episodes exceeding 60, 80, 100, and 122 ppb, respectively associated with the winter monsoon types, which accounted for 69, 57, 55, and 33 percent of the total episodes. The episodes of the two most abundant types C and NE accounted for almost 60% of the total episodes. It is worth to note that high concentration episodes exceeding 100 ppb have the highest chance to occur in the winter monsoon synoptic types and typhoon.

## 5. Discussion

Through synoptic meteorological diagnosis, we are able to identify several transport patterns and regions of ozone production associated with ozone episode occurrence. In this section we perform the analysis, with illustrated typical episode examples on the three kinds of pollutant transport and photochemical formation processes, which are the causes of majority of ozone episodes in Hong Kong. They are long-range transport of pollutant from distant sources through the Asian mainland, short-range transport of pollutant from neighborhood cities in PRD region, as well as local transport of pollutant within the territory of Hong Kong and subsequent photochemical ozone formation.

### 5.1 Long-Range Transport of Pollutants and Photochemical Ozone Formation

The long-range transport of ozone and pollutants from upwind distant sources of the East Asian region induces a strong impact on the atmospheric environment and the occurrence of ozone episode in South China. This kind of

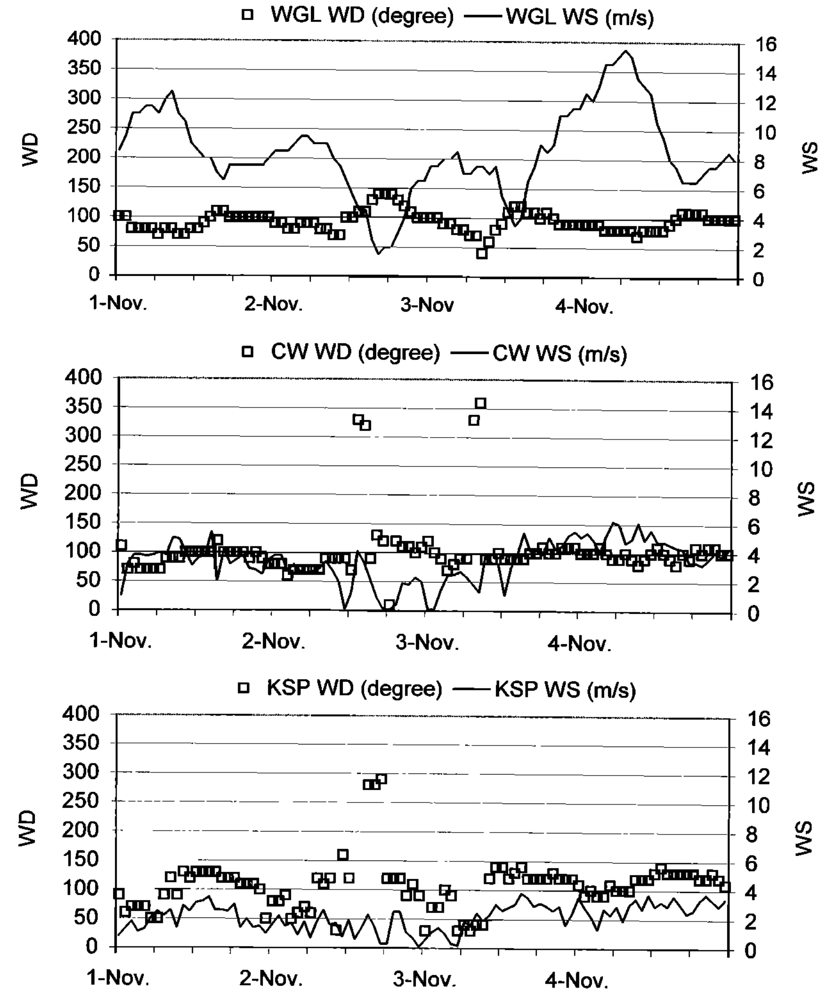


**Figure 2c.** The hourly time series of wind speed and direction from November 1 to 4, 1994.

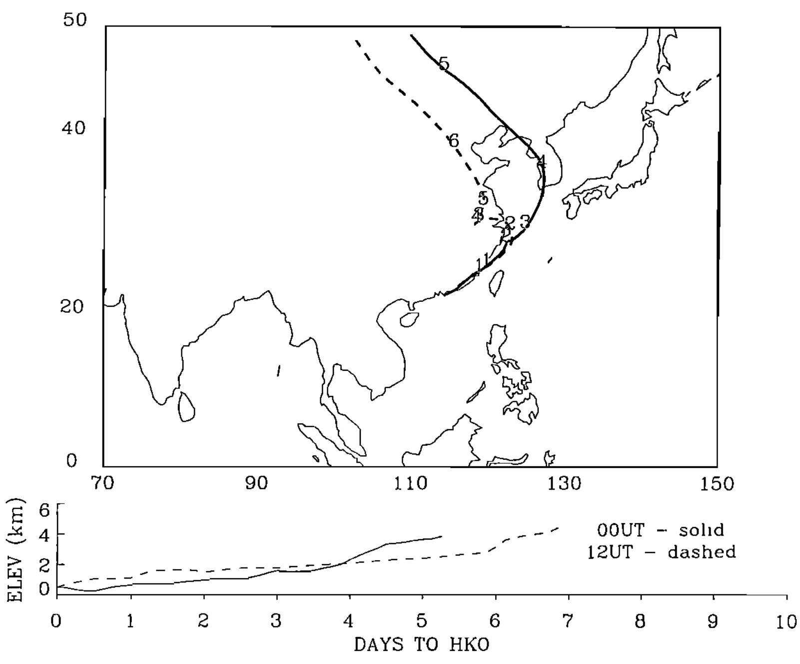


**Figure 2d.** The typical back air trajectories on November 4, 1994, ending at HKO and 0.5 km altitude.

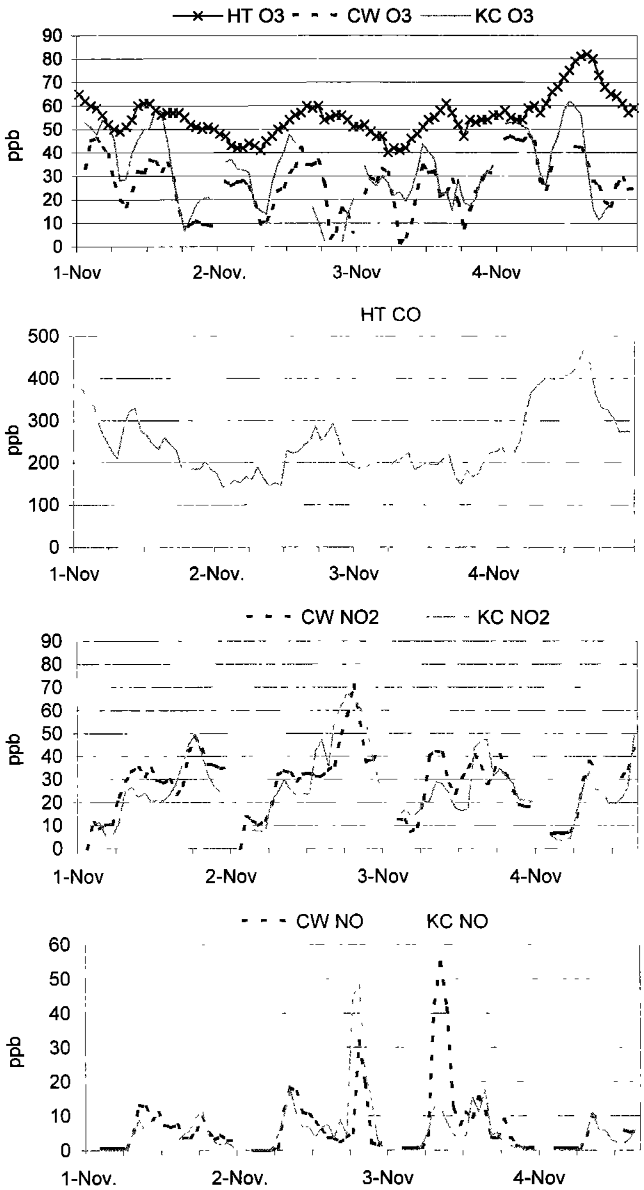


**Figure 2e.** The hourly time series of ozone, CO, NO, and $NO_2$ concentrations from November 1 to 4, 1994.

transport process is commonly observed during the continental outflow accompanied with winter monsoon and is reflected by an unique variation of ozone concentration related to synoptic patterns N, NE, and E episodes. These episodes feature a consistently high ozone level along with elevated CO level at night in the upwind background monitoring station, follow by a sharp rise of concentration in the middle of the day, and then a special early morning ozone peak in the urban and industrial stations. They often occur when there is strong surface wind from the northeast and east directions to Hong Kong. They are more frequent from late summer to early spring (from late September to the end of March), and their presence significantly influences the overall diurnal ozone variation in the territory. *Chan et al.* [1998a] had reported similar ozone behavior in their analysis of the average diurnal ozone variation for the autumn, winter, and spring seasons.

A typical case observed on November 1 to 4, 1994, is analyzed below. Figure 2 shows the daily weather maps, the streamline charts, and the hourly time series of wind speed and direction, ozone, CO, NO, and $NO_2$ concentrations recorded in HT, CW, and KC stations. The synoptic condition of these days were dominated by a series of moderate and weak continental anticyclones locating and moving along the northwestern continental mainland and northeastern part of China (types N, NE, and E respectively) (Figure 2a). This resulted in a general northeasterly airflow and surface wind along the coast of Asian continent, and air mass started to curve toward easterly in the southeast China region (Figure 2b). In Hong Kong the prevailing wind was mainly from the east (Figure 2c). Figure 2d presents the 10-day back air trajectories for November 4 ending at HKO and 0.5 km altitude. The trajectories agree with the streamline charts in these synoptic patterns. They are more useful in this case since they are able to provide information on the history of the air masses. The trajectories demonstrated that the air masses were originated from northern China, and then traveled through Mainland China and the coastal areas of the East China Sea near southern Japan. They continued to flow along the Taiwan Straits to approach the coastline of southern China and Hong Kong. The air masses were continental in nature with some modifications by the underlying land and sea surface during their journey. They were thus aged in nature. The concentration level of CO (250–450 ppb daily maximum) record in the remote HT station (Figure 2e), which received the easterly air masses from the sea, tended to support our above argument. This CO level distinguished the air mass from the one contaminated by urban emission with very recent history, which should have higher CO (in ppm level), and the one from the Pacific Ocean, which should have much lower CO.

There was only relatively limited fluctuation in the minimum ozone concentration at night in the remote upwind station HT. Note that the minimum hourly ozone concentration in the upwind remote station HT was always higher than 40 ppb, which then increased in the daytime and attained the maximum at afternoon. The peak concentration of ozone (85 ppb) occurred on November 4 (Figure 2e) coinciding with the maximum CO and the high wind speed. In the urban stations CW and KC the maximum ozone concentration, about the same level as that in the HT station (Figure 2e), was consistently observed at night or early morning coincided with the minimum NO. Also coinciding with rush hour periods, the ozone level dropped as the CO and NO level rises. These phenomena indicate that the ozone is originated from sources outside Hong Kong, and it is suppressed in the urban areas by the fresh NO emission.

There is limited direct emission source in the immediate upwind neighborhood in the northeastern and eastern directions of Hong Kong. The high level of background ozone concentration observed in the non-photochemical-active period (overnight), the flow patterns, and the subsequent ozone elevation in the daytime tend to suggest that these ozone episodes are related to the long-range transport of ozone and precursors as well as local photochemical ozone formation. The possible source regions may include the coast of Mainland China, the coastal areas of southern Japan, Taiwan, and southeastern China. As the air masses flow across these areas, they pick up anthropogenic pollutants, and ozone is being produced during the transportation of aged air.

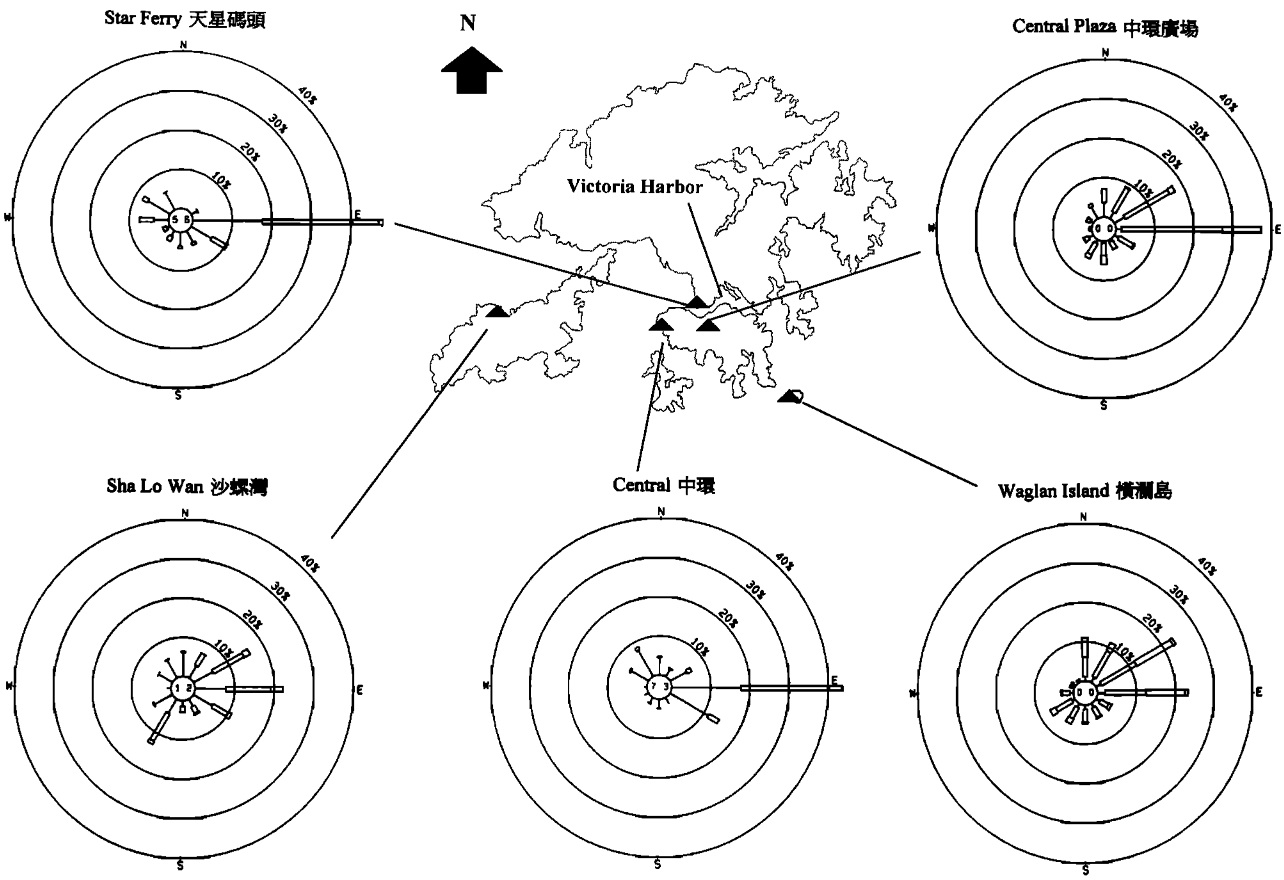


**Figure 3.** The windroses of selected meteorological stations along the Victoria Harbor for 1996.

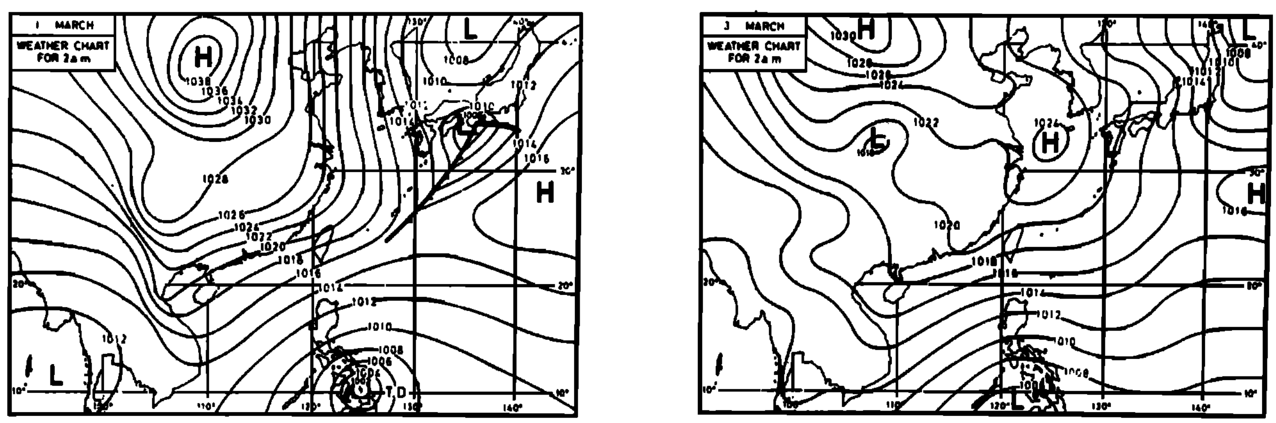


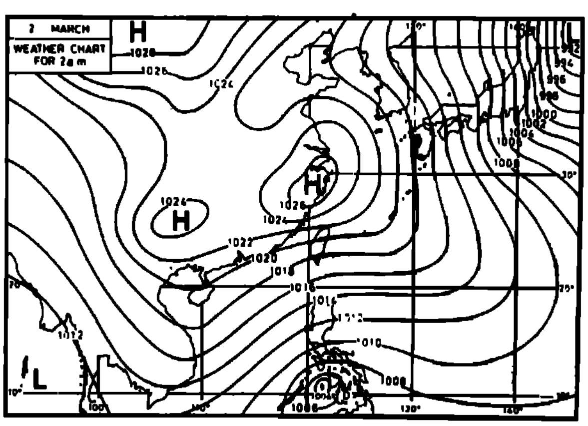


**Figure 4a.** The daily weather maps from March 1 to 3, 1996.

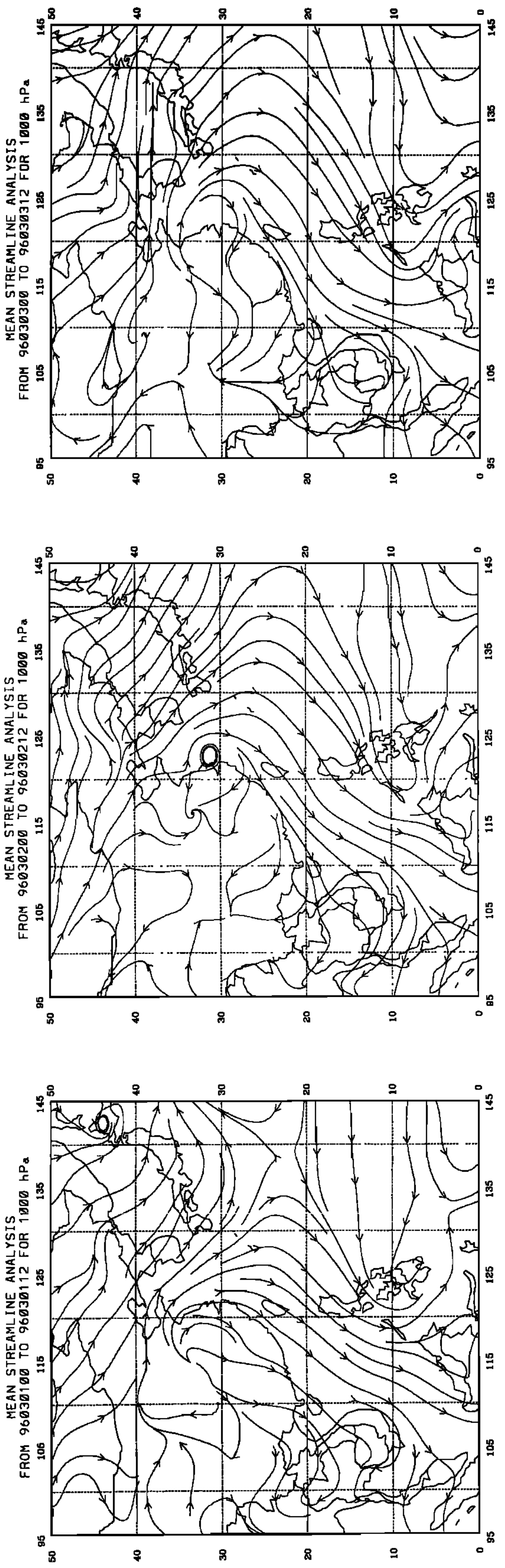


**Figure 4b.** Same as Figure 4a, but for the streamline charts.

*Akimoto et al.* [1996] had shown that, by the surface ozone measurements (September to October 1991) at three remote stations in southern Japan and Taiwan, continental air masses which were originated from northwestern Asia and passed through the high anthropogenic emission region of East Asia contained high concentration of ozone. In Europe, relatively high ozone level found at non-photochemical-active period (midmorning) is reported to be indicative of ozone transport from continental sources [*Colbeck and Harrision*, 1985].

The impact of this kind of long-range transport of background ozone and pollutants on local ozone level is especially dominant when background ozone is combined with the ozone formed from emissions from metropolitan Hong Kong. Ozone levels are then enhanced by the local-scale transport of pollutants and elevated photochemical processes. This will be analyzed in the next case.

### 5.2. Local Transport of Pollutants and Local Photochemical Ozone Formation

Local photochemical formation and accumulation of ozone are important causes of ozone episodes in Hong Kong. In most cases this is strengthened by complex transport pattern induced by the local topography. As shown in Table 2, the frequencies of occurrences of elevated ozone episodes per year (>80 ppb) found in the rural districts, especially those in the downwind western or northwestern sides of the territory (SLW and YL), are much higher than those observed in the upwind metropolitan districts. This tends to suggest that a large numbers of episodes are a result of the transport of pollutants emitted from the upwind local metropolitan areas with urban commercial and industrial activities, and subsequent photochemical ozone formation, as there is comparatively less ozone precursor emission in these districts. This phenomenon is more apparent in the SLW station, which is in the downwind side over 70% of the year as indicated by the prevalent wind. In fact, the highest frequency of ozone episodes per year (111 days >60 ppb) had been recorded in the downwind station SLW although the available ozone data for analysis were only for 1996. The local transport processes created by the topography of Hong Kong enhance the transport of pollutants and the subsequent photochemical ozone formation in this station.

SLW is situated at about 30 km on the western side of the territory (Figure 1). It is about 30 km downwind of the major emission areas on both sides of the Victoria Harbor. In 1994 there were a total of 148,064, 80,075, and 16,556 tones of $NO_x$, CO, and VOC, respectively, emitted from Hong Kong (EPD, private communication, 1996). Most of these pollutants are emitted from the metropolitan areas on both sides of the Victoria Harbor. Mountains on both sides of Victoria Harbor create a channeling effect that forces prevailing winds to turn easterly into the harbor (Figure 1) [*Yeung et al.*, 1990; *Chan et al.*, 1998a]. Figure 3 presents the windroses of some selected meteorological stations along Victoria Harbor for 1996. The predominant frequencies of surface winds in the easterly direction for Central Plaza (CP), Star Ferry (SF), and Central (CE) stations clearly demonstrate the channeling effect. Such effect enhances the transport of pollutants to the downwind locations. The local photochemical ozone formation in the transported air favors the subsequent ozone accumulation. The effect of these processes are more apparent

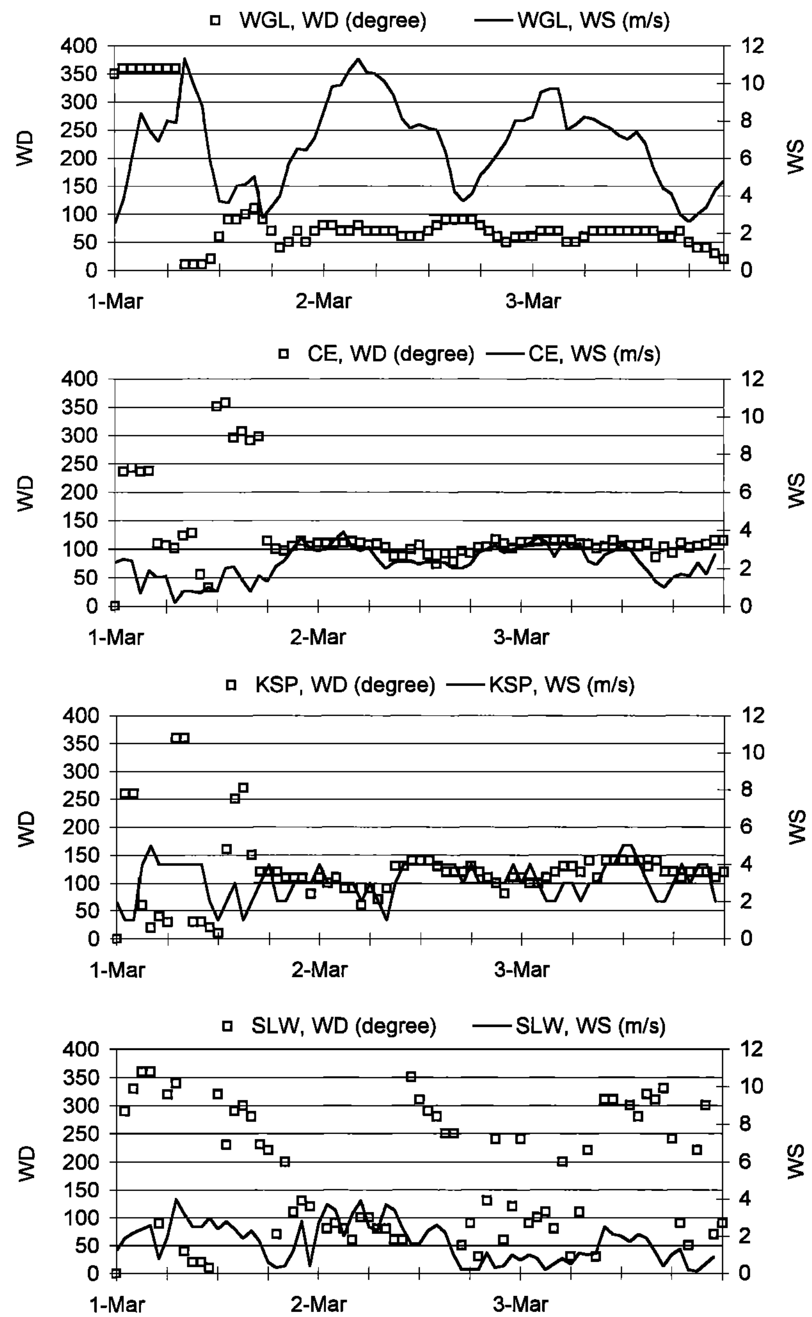


**Figure 4c.** The hourly time series of wind speed and direction from March 1 to 3, 1996.

when the synoptic patterns are moderate N, weak NE, E, and P. The general northeast, east, and southeast prevailing winds associated with these patterns are then channeled into easterly. In addition, the relatively weaker wind accompanying these situations favors the subsequent photochemical formation and accumulation of ozone downwind under favorable weather condition.

Figure 4 analyzed a typical case from March 1 to 3, 1996. The synoptic situation on March 1 was dominated by a moderately high pressure centered over northwestern China (moderate N), which moved in the southeast direction and then weakened in strength to change to synoptic type NE on the following 2 days (Figure 4a). This resulted in a flow of air masses from the central Asian continent along the coastal region of Mainland China as northeast wind (Figure 4b). In Hong Kong the prevailing wind was mainly from the general northeast direction as reflected by the wind direction in Waglan Island. The channeling effect was clearly demonstrated by the recording of easterly winds along both sides of the harbor in CE and KSP stations (Figure 4c). The accompanying wind speeds in these days were low, usually below 8 m/s. This is especially true in the downwind SLW station where it was always less than 4 m/s and the wind direction is more variable.

The inflow of high ozone and CO is reflected by the relatively stable concentration in the upwind remote HT

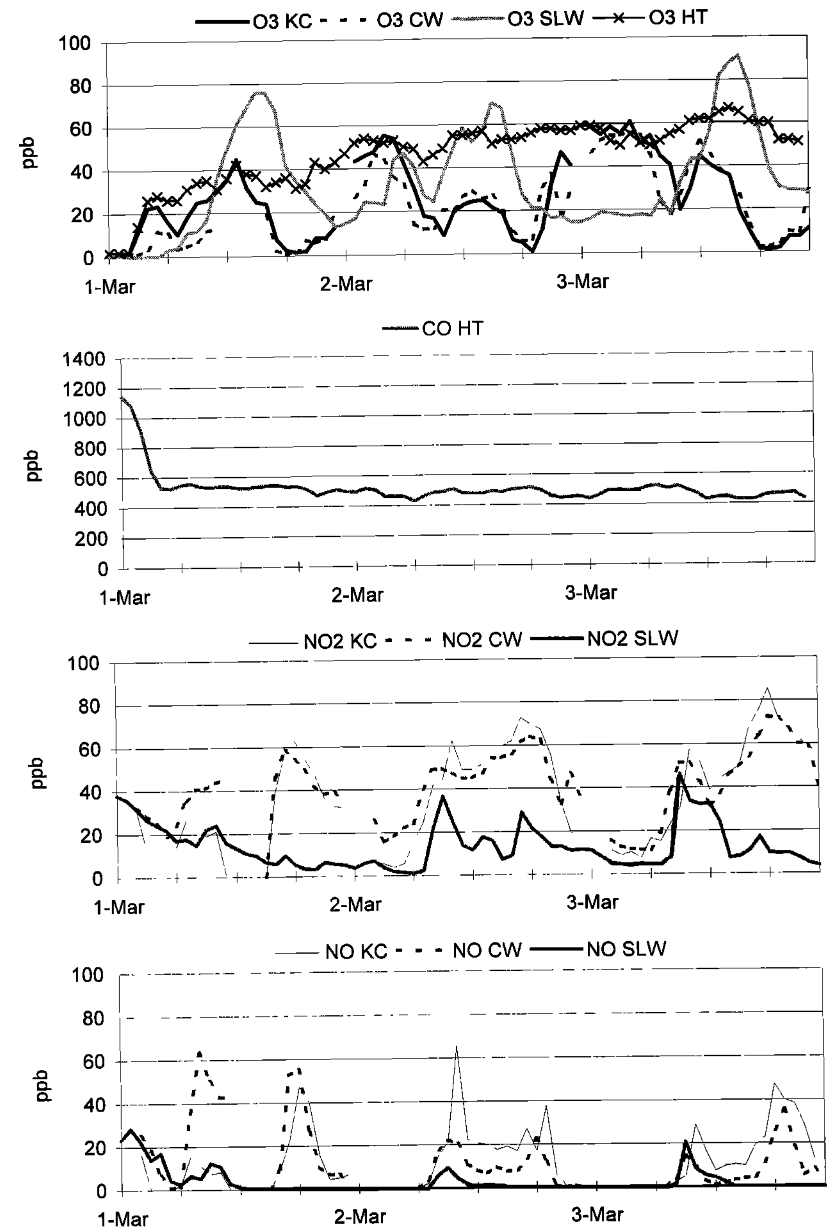


**Figure 4d.** Same as Figure 4c, but for the ozone, CO, NO, and $NO_2$ concentrations.

station despite the sharp variation in the very early morning on March 1 (Figure 4d) when the wind was from the northwest. This suggests that the pollutant inflow from farther upwind in the northeastern direction such as the one presented in the last case also plays an important role in this episode. Ozone in the urban (CW) and industrial (KC) stations had a lower level. It showed a bimodal pattern with maximum concentration occurring in the early morning coincident with minimum NO and minimum ozone coincident with highest NO. The highest NO concentration coincided with the peak traffic in rush hours. This is due to the titration effect of ozone by freshly emitted NO from traffic around the urban stations CW and KC. The chemical titration of ozone by NO occurs quite fast in the atmosphere, and this reaction temporarily transfers ozone to $NO_2$ before the subsequent photochemical formation of ozone from $NO_2$. The channeled easterly wind (Figure 4c) within the harbor, however, blows the pollutants downwind and prevents the pollutants from accumulating in these two districts. Note that the afternoon peak ozone concentration was not observed in the upwind stations CW and KC, and instead the peak was replaced by $NO_2$ concentration. Such observation tends to support our argument. The titration effect is comparatively less in the downwind station SLW. The peak ozone concentration in SLW was the highest, and it increased from the morning hours to reach its peaks in the late afternoon coincident with the maximum temperature in these days. Moreover, there is much lower concentration of $NO_x$ than the two upwind metropolitan stations, especially for NO (Figure 4d) in the daytime. This leads us to suggest that there is local transport of ozone precursors to the downwind remote area and in situ photochemical ozone formation accompanying the aging air

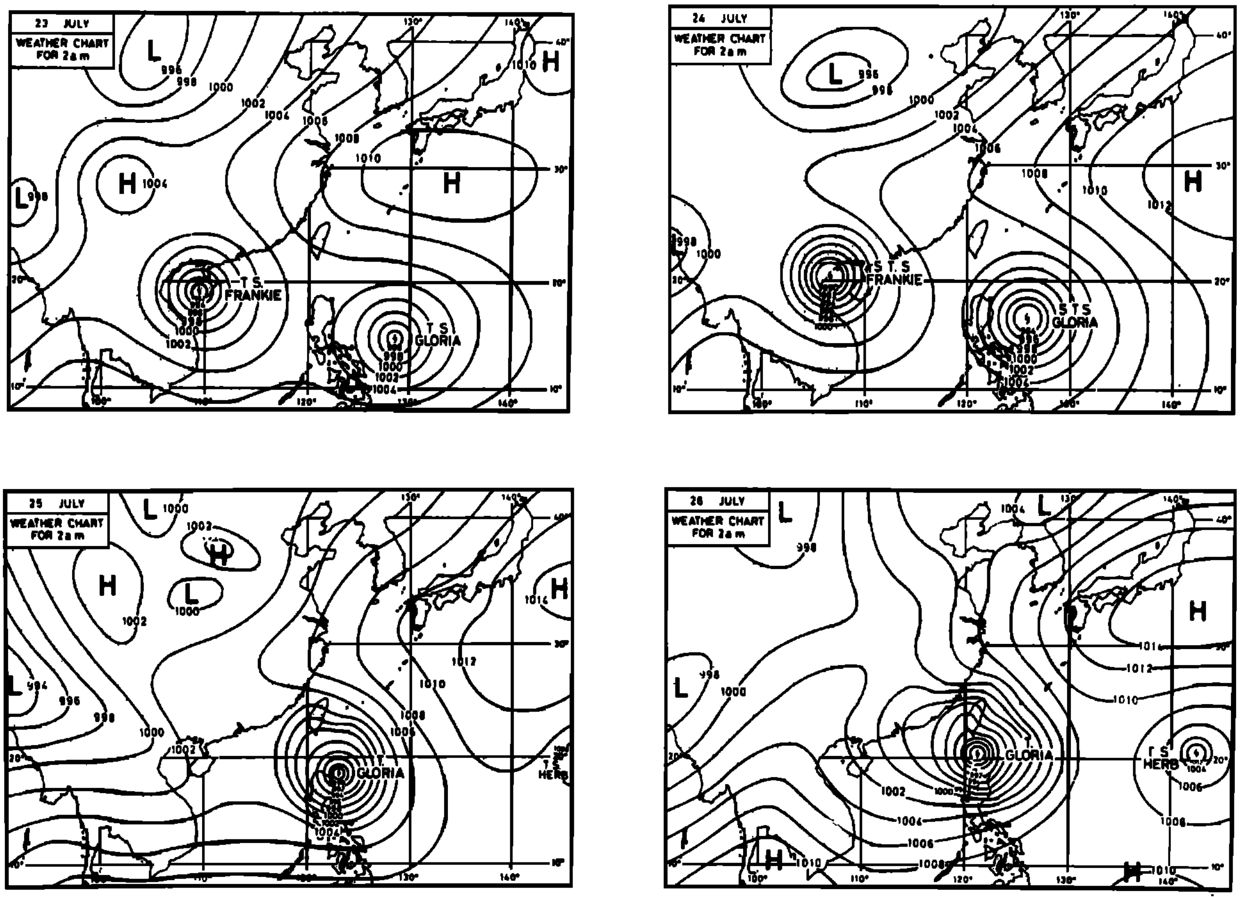


**Figure 5a.** The daily weather maps from July 23 to 26, 1996.

mass. The maximum hourly ozone concentrations of these days were 76, 71, and 91 ppb in SLW despite only moderate high temperature (24°-26 °C, daily average) recorded during this period.

### 5.3. Short-Range Transport of Pollutants and Photochemical Ozone Formation

Ozone episodes associated with synoptic pattern wN, C, H, and T are marked by weak regional flow with clam condition or with weak prevailing winds from the general north and northwest direction. The winds always bring in anthropogenic pollutants from the neighborhood of Hong Kong. There are flourishing urban cities and industrial centers within our close proximity in the Guangdong Province and the Pearl River Delta in southern China (Figure 1). The nearest Chinese city, Shenzhen Special Economic Zone (SEZ), with 4 million people is roughly 35 km north from the urban center of Hong Kong. The central city of Guangdong Province, Guangzhou is 120 km northwest of Hong Kong. The populated urban centers, Zhuhai SEZ and the Portuguese colony, Macau, are located about 70 km in the west. In 1987 a total of 80 and 1.5 GgN of $NO_2$ were emitted in Guangdong Province and Macau, respectively [*Akimoto and Narita*, 1992]. The short-range transport of ozone and pollutants from these industrial and urban centers in the Pearl River Delta and the Guangdong Province greatly influences the occurrence of high ozone episodes in Hong Kong. This is especially true when the meteorological and weather conditions associated with these synoptic patterns are favorable for photochemical ozone formation. The superposition of these two ozone sources very often leads to territory-wide and extremely high ozone episodes in Hong Kong.

Ozone episodes associated with the approaching typhoon (type C) are most critical among these synoptic patterns. It is because the transport of pollutants is accompanied by the sharp change of wind direction together with favorable photochemical ozone formation condition. Figure 5 presents an extreme case from July 23 to 26, 1996. During this period, southeast China was under the influence of two tropical typhoons Frankie and Gloria (Figure 5a). On the first 2 days, Hong Kong was on the eastern side of Frankie and under the influence of its outer shirt on the east direction (Figure 5b). The cyclonic motion of the typhoon brought in fresh gusty winds (Figure 5c) from the sea surface which resulted in occasional heavy showers. The inflow of the clean air masses from the South China Sea and the scavenging and washing out effects caused the pollutants to reach a low concentration level (Figure 5d).

As Frankie moved away from Hong Kong and dissipated over the land, Gloria moved closer to southeast China on July 25 and 26 (Figure 5a). Hong Kong was then on the left side of the typhoon. The cyclonic motion of Frankie turned the winds to flow from the northwestern direction and brought hot continental air masses into Hong Kong. The influence of the cyclonic motion is clearly demonstrated by the anticlockwise appearance of the streamline charts (Figure 5b) and the sharp

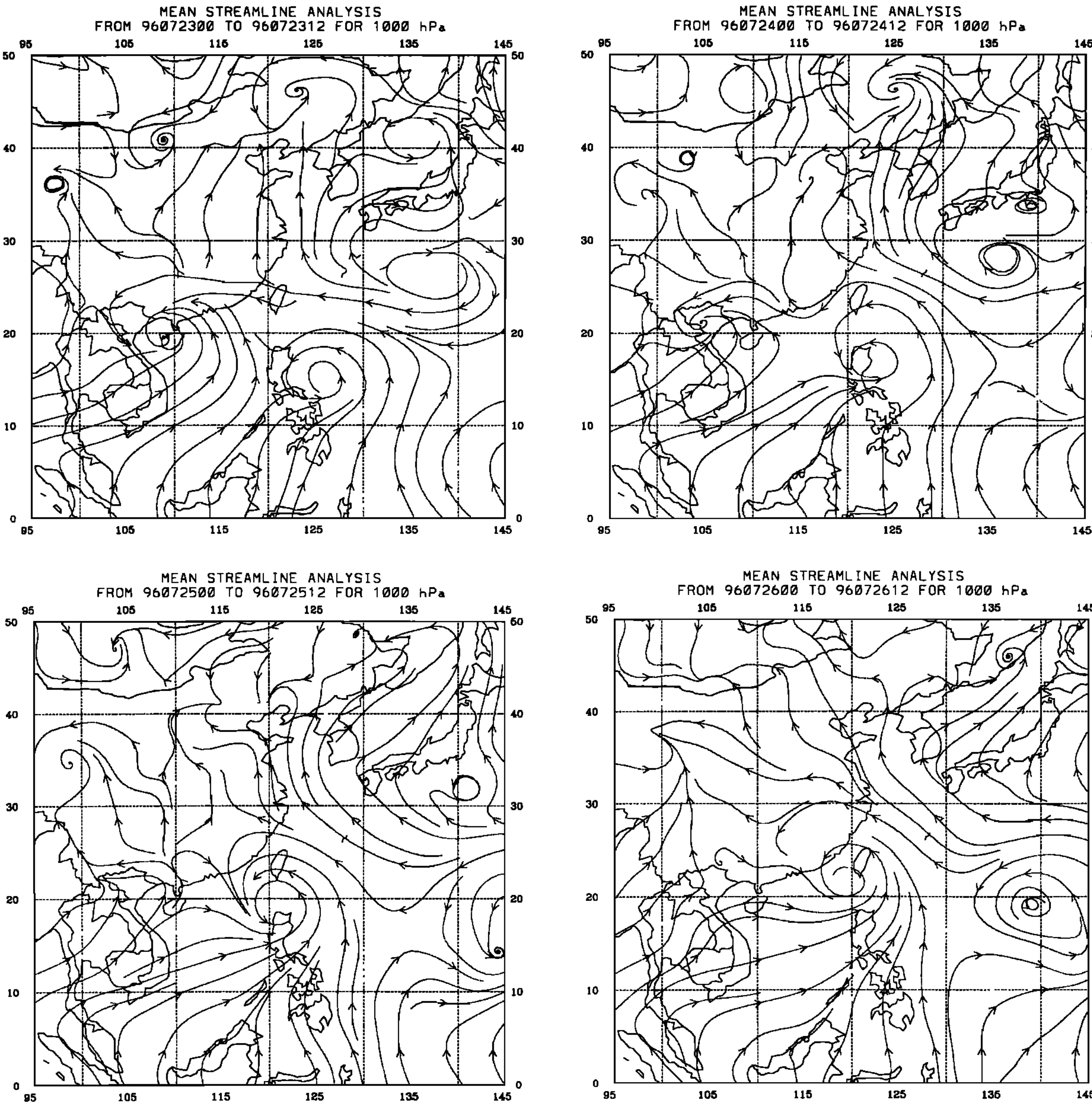


**Figure 5b.** Same as Figure 5a, but for the streamline charts.

change of surface wind directions to the northwestern direction (Figure 5c) at late July 24 and early July 25. The wind remained consistent when the typhoon moved closer on the following 2 days. On July 25 and 26 the subsiding motion of the outer region of Gloria resulted in a clear sky. It was dominated by low percentage of cloud cover (29 and 65%, respectively). The subsiding motion also caused a shallow boundary layer in Hong Kong. The mixing heights as determined by radiosonde temperature profile at King's Park HKO station (Figure 1) were very low. They reached only 406 and 507 m in the morning at 0800 local standard time and daily maximum of 1150 and 991 m on July 25 and 26, respectively. These mixing height values were low compared with the ones commonly observed in this month. The vertical temperature profiles recorded at night (2000 local standard time) showed that the lower atmosphere was even more stable with temperature increased with height up to 400 m aboveground. The low mixing height indicates that the boundary layer was capped by an inversion at the top of the boundary layer in these 2 days when the typhoon approached closer to Hong Kong. It was also noted that the wind speed was very low (<4 m/s) in less ventilated times (Figure 5c). The maximum hourly solar radiation of these 2 days reached above 730 and 850 MW/m$^2$ (Figure 5e). Under these conditions the highest temperature of the month (35°C) was recorded on July 26 (Figure 5e). These meteorological conditions favor subregional as well as local photochemical formation and ozone accumulation.

The airflow pattern caused an inflow of pollutants from neighboring cities in Guangdong Province and the PRD cities. As a consequence, there was sharp and simultaneous increase of CO in HT and KC accompanying the change of wind direction at late July 24 and early 25. Also, the diurnal variation pattern of CO and $NO_2$ in these days indicated that there was a gradual accumulation of pollutants in the daytime. CO in KC reached almost 10,000 ppb and around 10 times

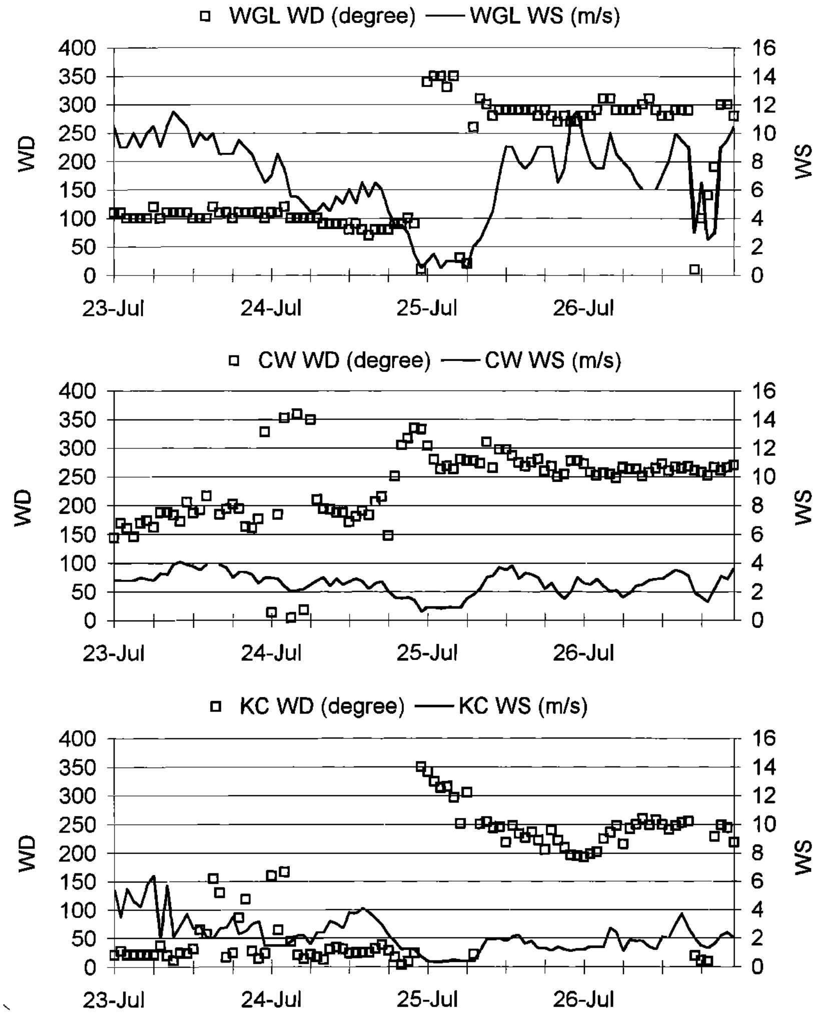


**Figure 5c.** The hourly time series of wind speed and direction from July 23 to 26, 1996.

that in HT. This high CO level observed in these stations should indicate that air mass was rich in anthropogenic pollutants and had picked up substantial emissions from the PRD cities and metropolitan Hong Kong inducing a buildup of pollutants in the shallow boundary layer. Ozone showed a sharp rise in concentration from morning to reach the peaks in late afternoon (Figure 5d) coinciding with the CO peaks in these 2 episodic days. We also noted that the increase and high level of ozone were mainly found during the photochemical active period. Figure 5d and 5e show that the rise of ozone coincided with the appearance of solar radiation. The sharp ozone increase occurred simultaneously with solar radiation and temperature from around 0900 local standard time to attain its peak level coinciding with the highest temperature period at around 1500 and 1600 local standard time (LST). The highest ozone was found in the upwind SLW station in the west, and the lowest one was recorded in the downwind HT station. The maximum hourly ozone concentration of these 2 episode days attained a range of 80 to 160 ppb with high concentration also found in the upwind station in the north (YL). In YL the ozone peak occurred at 1500 LST an hour before that in SLW and KC and 2 hours before the second peak of HT. These time delays of ozone peak between the upwind and the downwind stations together with the spatial distribution of ozone concentrations highlight the importance of the short-range transport of pollutants from the northwestern direction.

The subsiding motion associated with typhoon is known to be able to bring ozone from the stratosphere or upper troposphere to ground level. The ozone may combine with the ozone photochemically produced in the boundary layer to cause an ozone episode. In our case the rate of ozone increase was substantial, and the time delays of ozone peak were relatively short. These might have implied that there were some contributions of stratospheric or upper tropospheric ozone to the ground level. However, based on the available meteorological and chemical data, we cannot substantiate this hypothesis. This would be subject to further analysis.

## 6. Conclusion

In this study, the effects of meteorology and air pollutant transport on ozone episodes in coastal South China are investigated through assessing the limited but valuable database of ozone and its precursors at various monitoring stations in Hong Kong. The links between the synoptic-scale flow pattern, the mesoscale weather phenomenon, the local micrometeorology, and the occurrence of ozone episodes are analyzed with the combine use of surface pressure patterns, streamline charts, and prevalent winds. The major source

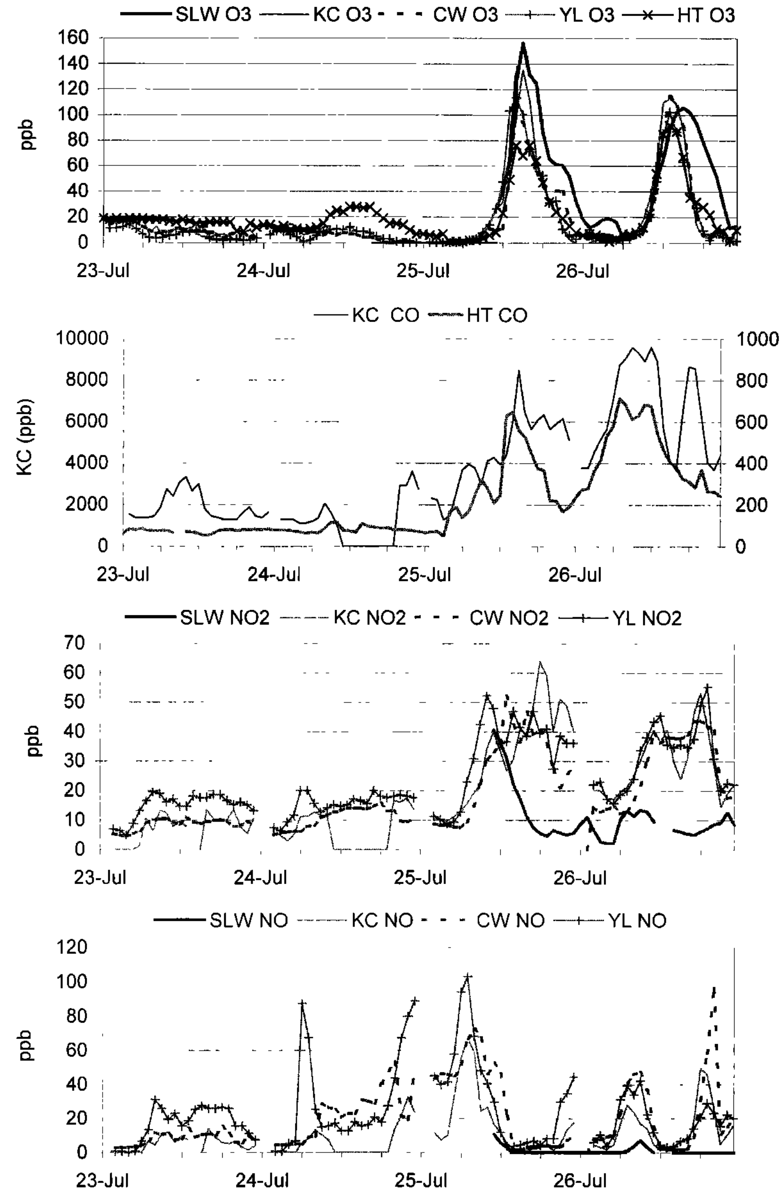


**Figure 5d.** Same as Figure 5c, but for the ozone, CO, NO, and $NO_2$ concentrations.

regions of ozone production, the scales of pollutant transport, and the photochemical ozone formation accompanying the meteorological patterns are discussed with illustrative episodes.

Using available data from the HKPolyU and EPD network, we reveal that high frequencies of ozone episodes and elevated ozone concentration are found in most urban areas, industrial areas, new towns and especially in the rural and remote districts of Hong Kong. Meteorological and synoptic conditions are found to have strong effects on the transport of pollutants to the territory and the occurrence of ozone episodes. Synoptic patterns associated with the occurrence of ozone episodes are classified into nine types. They are northerly (N), weak northerly (wN), northeasterly (NE), easterly (E), Pacific ridge (P), cyclone (C), high-pressure cell (H), trough (T), and southerly (S). The patterns associated with winter monsoon and traveling cyclones are found to be most conducive to the occurrence of ozone episodes. The causes of ozone episodes can be summarized as long-range transports of pollutant from distant sources in East Asia; local transport of pollutants upwind from metropolitan areas of Hong Kong; short-range transport of pollutant from the neighborhood metropolitan and industrial areas in South China and the subsequent photochemical ozone formation. Long-range transport of ozone and pollutants from the aged continental air mass contributes to substantial cases of episodes in the upwind remote areas. The possible source regions of this ozone may include the Asian continent, the coastal areas of southern Japan, and Taiwan. This high inflow of background ozone together with the elevated ozone enhanced by the channeling effect and local transport causes the highest frequency of episodes found in the downwind western side of the territory. The short-range transport of ozone and precursors from the industrial and urban centers in the Pearl River Delta region and Guangdong Province is another source of ozone. The high ozone content from these

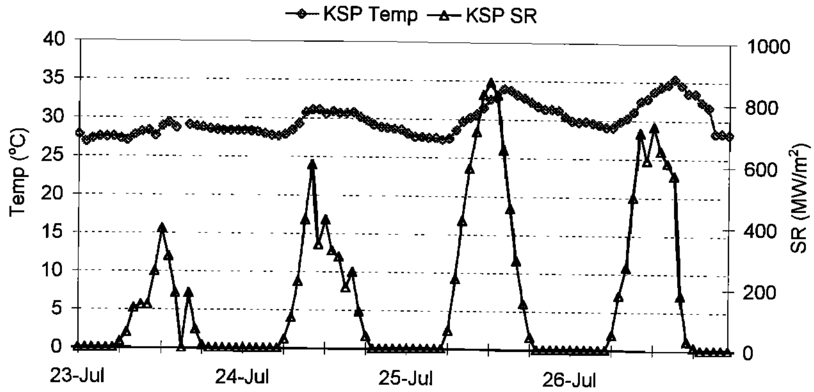


**Figure 5e.** Same as Figure 5c, but for the temperature and solar radiation.

areas, when combined with the one formed from local sources often leads to territory-wide and extremely high ozone episodes in Hong Kong.

The large-scale and mesoscale transport of pollutants and ozone formation processes associated with the winter monsoon and typhoon should imply that the territorial wide ozone pollution observed in Hong Kong should also occur in South China such as in PRD cities. Apart from the consideration of local ozone precursor emission and ozone formation, our analysis shows that the examination of meteorology and trans-boundary ozone and precursor transport are needed to successfully formulate ozone control strategy to be implemented in South China and Hong Kong. In addition, our meteorological and ozone episode diagnosis have demonstrated that the "background" outflow of Asian pollutants can be significantly modified on its way to the Pacific Ocean through the fast growing Pearl River Delta cities such as Hong Kong.

**Acknowledgments.** The authors would like to thank the Environmental Protection Department and Hong Kong Observatory and the Hong Kong Polytechnic University Background Air Quality Monitoring Station for providing the necessary data, and the GTE Project Office for supplying the streamline charts. This study is supported by a Hong Kong Polytechnic University research grant and a grant from the Research Grant Council of Hong Kong. The authors would like to thank the reviewers for the helpful comments.

## References

Akimoto, H. and H. Narita, Distribution of $SO_2$, $NO_x$ and $CO_2$ emissions from fuel combustion and industrial activities in Asia with 1° × 1° resolution, *Atmos. Environ., Part A, 28*, 213-225, 1992.

Akimoto, H., et al., Long-range transport of ozone in the East Asian Pacific Rim region, *J. Geophys. Res., 101*, 1999-2010, 1996.

Angle, R. P., and H. S. Sandhu, Urban and rural ozone concentrations in Alberta, Canada, *Atmos. Environ., 23*, 215-221, 1986.

Bower, J. S., et al., Surface ozone concentrations in the U.K., in 1987-1988, *Atmos. Environ., 23*, 2003-2016, 1989.

Chan L. Y., C. Y. Chan and Y. Qin, Surface ozone pattern in Hong Kong, *J. Appl. Meteorol. 37, 10*, 1151-1165, 1998a.

Chan, L. Y., H. Y. Liu, K. S. Lam, T. Wang, S. J. Oltmans, and J. M. Harris, Analysis of the seasonal behavior of tropospheric ozone at Hong Kong, *Atmos. Environ. 31*, 159-168, 1998b.

Chin, P. C., Climate and weather, in *A geography of Hong Kong*, edited by T. N. Chiu and C. L. So, 403 pp., Oxford Univ. Press, New York, 1986.

Colbeck, I. and R. M. Harrison. The photochemical pollution episode of 5-16 July 1983 in north-west England, *Atmos. Environ., 19*, 1921-1929, 1985.

Environmental Protection Department (EPD), Air quality in Hong Kong: Results from the air quality monitoring network, Hong Kong Govt. Printer, Hong Kong, 1994.

Fast, J. D., and C. M. Berkowitz, Evaluation of back trajectories associated with ozone transport during the 1993 North Atlantic Regional Experiment, *Atmos Environ., 31*, 825-837, 1997.

Hanna, S. R. and J. C. Chang, Relations between meteorology and ozone in the Lake Michigan Region, *J. Appl. Meteorol., 34*, 670-678, 1995.

Heywood, G. S. P., Surface pressure-patterns and weather around the year in Hong Kong, *Tech Memo. 6*, R. Obs., Hong Kong, 1953.

Jacob, D. J., J. A. Logan, and P. P. Mupti, Effects of rising Asian emissions on surface ozone in the United States, *Geophys. Res. Lett., 26*, 2175-2178, 1999.

Jaffe, D., T. et al., Transport of Asian air pollution to North America, *Geophys. Res. Lett, 26*, 711-714, 1999.

Lippmann, M., Health effects of tropospheric ozone, *Environ. Sci. Technol., 25*, 1954-1962, 1991.

Liu, H. Y., S. J. Oltmans, L. Y. Chan, J. M. Harris and W. L. Chang, On the springtime high ozone peak events in the lower troposphere over Hong Kong and the biomass burning in Southeast Asia, *Atmos. Environ. 33*, 2403-2410, 1999.

Logan, J. A., Ozone in rural areas of United States, *J. Geophys. Res., 94*, 8511-8532, 1989.

Miller, J. M., J. L. Moody, J. M. Harris, and A. Gaudry, A 10-year trajectory flow climatology for Amsterdam Island, 1980-1989, *Atmos Environ., Part A, 27*, 1909-1916, 1993.

Moody, J. L., S. J. Oltmans, H. Levy II, and J. T. Merrill, Transport climatology of tropospheric ozone: Bermuda, 1988-1991, *J. Geophys. Res, 100*, 7179-7194, 1995.

National Research Council (NRC), *Rethinking the Ozone Problem in Urban and Regional Air Pollution*, 487 pp., Nat. Acad. Press, Washington, D. C., 1991.

Parrish, D. D., J. S. Holloway, M. Trainer, P. C. Murphy, G. L. Forbes, and F. C. Fehsenfeld, Export of North American ozone pollution to the North Atlantic Ocean, *Science, 259*, 1436-1439, 1993.

United Kingdom Photochemical Oxidants Review Group (PORG), Ozone in the United Kingdom, final report, AEA Harwell Lab., Didcot, England, 1990.

Wang, T., K. S. Lam, L. Y., Chan, Z. L. Cheng, M. Anson and M. A. Carroll, Trace gas measurement during the periods of outflow from the Asian continent: Results from a Hong Kong site during PEM-WEST B, *J. Geophys Res., 102*, 28,575-28,588, 1997.

Wang, T., K. S. Lam, Agatha S. Y. Lee, S. W. Pang, and W. S. Tsui, Meteorological and chemical characteristics of the photochemical ozone episodes observed at a coastal location in Hong Kong, *J. Appl Meteorol. 37*, 1167-1178, 1998.

Yeung, K. K., W. L. Chang, B. Wan, F. Kimura, and T. Yoshikawa, Simulation of boundary layer flow in Hong Kong, *Atmos. Environ Part A, 25*, 2161-2172, 1990.

C. Y. Chan and L. Y. Chan, Environmental Engineering Unit, Department of Civil and Structural Engineering, The Hong Kong Polytechnic University, Hung Hom, Hong Kong. (e-mail: 95982258r@polyu.edu.hk, celychan@polyu.edu.hk)

(Received March 10, 1999; revised February 21, 2000; accepted February 25, 2000.)